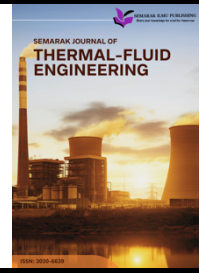




Semarak Journal of Thermal-Fluid Engineering

Journal homepage:
<https://semarakilmu.my/index.php/sjotfe/index>
ISSN: 3030-6639



Analysis of COVID-19 Aerosol Dispersion in a Car Cabin Due to Driver's Cough

Ridwan Abdurrahman¹, Nuraqilah Zahari², Ishkriyat Taib^{2,*}, Nabil Izzuddin², Peter Ting², Aiman Zuhdi², Ali Kamil Kareem³

¹ Mechanical Engineering Department, Universitas Riau, Pekanbaru 28293, Indonesia

² Faculty of Mechanical and Manufacturing Engineering, Universiti Tun Hussein Onn Malaysia, 86400 Parit Raja, Batu Pahat, Johor, Malaysia

³ Department of Biomedical Engineering, Al-Mustaqbal University College, Babylon, Iraq

ARTICLE INFO

Article history:

Received 10 March 2024

Received in revised form 18 April 2024

Accepted 7 May 2024

Available online 6 June 2024

Keywords:

Coronavirus; coughing; flow characteristics

ABSTRACT

The current coronavirus outbreak, attributable to SARS-CoV-2, has triggered widespread interest in the risk of infection associated with confined spaces. This study focuses on establishing a model for simulating the spread of COVID-19 within a car cabin due to a driver's cough using computational fluid dynamics (CFD) simulation in the ANSYS Fluent software. Previous studies have mainly focused on the transmission of the virus over large areas; however, attention has shifted to confined areas, including cars. This study fills this gap by modelling the flow regions, velocity, and pressure fields of virus-containing aerosols. This includes constructing a three-dimensional model of a car cabin and visualising cough droplet movement. While tracking the dispersal of viral particles, the discrete phase model was applied with the stipulation of boundary conditions to mimic real-life coughing. The verification used in the study was a grid independence test, after which the simulations examined the particle residence time, streamline, and velocity field in the car. Studies have shown that viral particles can persist in the air for quite a while and circulate to various parts of the car cabin, thus putting the occupants at a higher risk of infection. The streamline analysis revealed possible propagation routes and recirculation zones that may amplify the transmission from the driver to the rest of the car occupants. The velocity distribution emphasises the potential exposure risk. The findings of this study corroborate previous research on the increased exposure of COVID-19 car interiors, with particular emphasis on the transmission from the driver to the other occupants of the car. The outcomes of the research have drawn conclusions about the effectiveness of ventilation as well as other preventive measures to decrease the rate of airborne transmission in vehicles, thus responding to the objectives of the study.

1. Introduction

First recognised in December 2019 in Wuhan, China, Coronavirus Disease 2019 has already affected more than 3.5 million people worldwide and caused 243,401 deaths as of 5 May 2020. The

* Corresponding author.

E-mail address: iszat@uthm.edu.my

<https://doi.org/10.37934/sjotfe.1.1.2333a>

virus represents an airborne pathogen diffuse, as indicated by research, when an infected person speaks, breathes, coughs, or sneezes [1-3]. As it can be transmitted everywhere, it is difficult to avoid contact with such a pathogen. Some studies have supported that humidity, temperature, sunlight, and ventilation seem to be factors that influence the rapid spread of infection.

This study psychologically analysed the spread of COVID-19 due to the cough of a driver in a car by fluid dynamic analysis. The geometrical model of the study plans to include persons coughing in an automobile as the source of the virus. According to previous research, the species transport model, which involves the inclusion of three gases—oxygen (O_2), nitrogen (N_2), and water vapour (H_2O)—is activated [4, 5]. Air was the primary fluid in the computational domain. The conditions of the discrete phase model are rather different in such a way that particles at the edge of the patient's mouth have a state of escape, which involves particles passing through the boundary that it is part of, and those at the edge of the patient's body and all aside walls of the vehicle are in a trapped state, which means that these particles are stuck in these boundaries. To mimic the spread of COVID-19 through a cough, the discrete phase model was run using ANSYS Fluent software. The simulation illustrated the spread of virus particles in the air of a car's airflow over a specific time interval. The indirect responses of temperature, humidity, and rainfall to the spread of COVID-19 have been studied extensively, with the corresponding pollutant emissions being taken into consideration. The influence of ventilation on material emissions and the subsequent possibilities for infection spread have also been the object of multiple studies [6, 7]. The Institute of Occupational Safety and Health (NIOSH), which often ensures that workers do not have exposure to gas vapour in industries, including the oil and gas industries [8, 9], also mandates the use of this equipment.

Previous research, such as that conducted by the CFD Society of Canada, investigated airflow patterns and heat transfer in passenger cars [10]. Studies have examined the effectiveness of heating, ventilation, and air conditioning (HVAC) systems in maintaining comfortable climates inside cars. Factors such as HVAC inlet configuration, air temperature, and velocity were analysed to understand their impact on internal air circulation. Furthermore, research by Brown University has explored how airflow patterns inside a car may affect pathogen transmission [11-17]. Simulations conducted on a model car revealed that opening windows can significantly reduce the concentration of airborne particles exchanged between the occupants. Different combinations of open windows create distinct airflow patterns that influence exposure to the remaining aerosols. The geometry of the study involved modelling a passenger car with simplified representations of human occupants. The boundary conditions were set based on the experimental data to simulate realistic scenarios. This study aimed to provide insights into strategies for minimising the risk of COVID-19 transmission within confined spaces, such as cars. By integrating findings from previous studies and utilising advanced simulation techniques, this study seeks to enhance our understanding of COVID-19 transmission dynamics and inform preventive measures to mitigate its spread in enclosed environments.

2. Methodology

2.1 Geometry of the Cabin

The dimensions of the car model used in this study were inspired by previous research and are detailed in Table 1. The car model had the following dimensions: length of 2.5 meters, width of 1.2 meters, and height of 1.2 meters. The airflow rate within the car is set at 0.06 cubic meters per second (m^3/s), with an airflow speed of 1 meter per second (m/s). These parameters are crucial for accurately simulating the dispersion of virus-laden particles in a confined car interior, allowing for a realistic analysis of how a driver's cough spreads the virus throughout the vehicle.

Table 1
 Table of the geometry of the model

Parameter	Dimension
Length	2.5 m
Width	1.2 m
Height	1.2 m
Airflow rate	0.06 m ³ /s
Airflow speed	1 m/s

2.2 Discretization Technique

The flow characteristics and dispersion of breath and cough particles were modelled using commercial software to study the desired result. ANSYS FLUENT was used to simulate the airflow in the car and the dispersion of breath and cough particles. The main equations used in the CFD analysis are as follows: Eq. (1) and (3), respectively. These equations of motion can be used to predict the particle or aerosol trajectory in a discrete phase [18-20]. The trajectory of a particle, such as a droplet, can be predicted through the particle force balance in Eq. (4) and (5), respectively.

$$\text{Continuity equation: } \frac{\partial \rho}{\partial t} + \nabla \cdot (\rho v) = S_m \quad (1)$$

$$\text{Momentum equation: } \frac{\partial \rho}{\partial t} + \nabla \cdot (\rho v) = - + \nabla \cdot (\tau) + \rho g + F \quad (2)$$

$$\text{Energy: } \frac{\partial}{\partial t} (\rho E) + \nabla \cdot (v(\rho E +)) = \nabla \cdot (k_{eff} \nabla T - \sum h_i \cdot J_j + (\tau_{eff} \cdot \nabla)) + S_h \quad (3)$$

$$\frac{dup.}{dt} = F_d(u - u_p) + \frac{g_x(\rho_p + \rho)}{\rho_p} + F_x \quad (4)$$

$$F_d(u - u_p) = \frac{18\mu}{\rho_p d_p^2} \frac{C_d \cdot Re}{24} \quad (5)$$

2.3 Meshing of the Gas Mask Model

This study produced five types of meshes, each with a different number of grid nodes and elements, all of which were generated to guarantee the accuracy and reliability of the results. The first mesh had 516,672 grid nodes and 2,741,156 grid elements; therefore, it was the second smallest grid mesh. The second mesh increased these numbers to 614,481 grid nodes and 3,301,376 grid elements, respectively. The third mesh further refined the model with 717,041 grid nodes and 3,896,155 grid elements. The fourth mesh included 811,362 grid nodes and 4,444,880 grid elements, whereas the final mesh contained 915,374 grid nodes and 5,052,242 grid elements. Through the gradation of the mesh density, it was possible to thoroughly analyse the effect of the mesh size on the wave simulation and find a solution for the most efficient mesh configuration that could absorb the fluid effects and dispersion of particles inside the car model, as shown in Figure 1. Determining the mesh size and its implications in the simulation results is a very important step in validating the computational model used in this study.

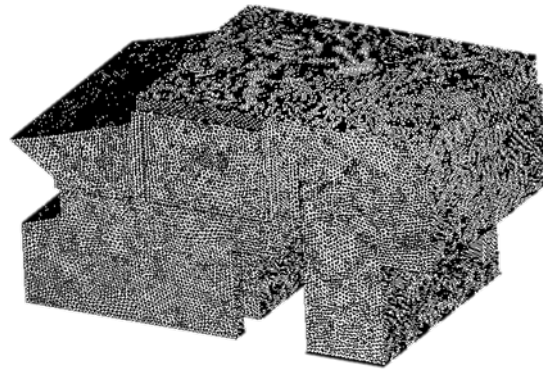


Fig. 1. Meshing generation for internal car cabin

2.4 Parameter Assumptions and Boundary Conditions

The boundary conditions used in the simulation are shown in Figure 2 and Table 2, where it is crucial to accurately model the spread of virus-laden particles in a car. The inlet, wall, and outlet boundary conditions are shown in Figures 2(a) 2(c), respectively. The inlet of the human mouth was simplified as a circle, whereas the outlet and wall boundaries were simplified as rectangles. The velocity of the car inlet was set as 1 m/s. The velocity of air from the human mouth was set at three different values: 1.3 m/s, 3.5 m/s, and 5 m/s.

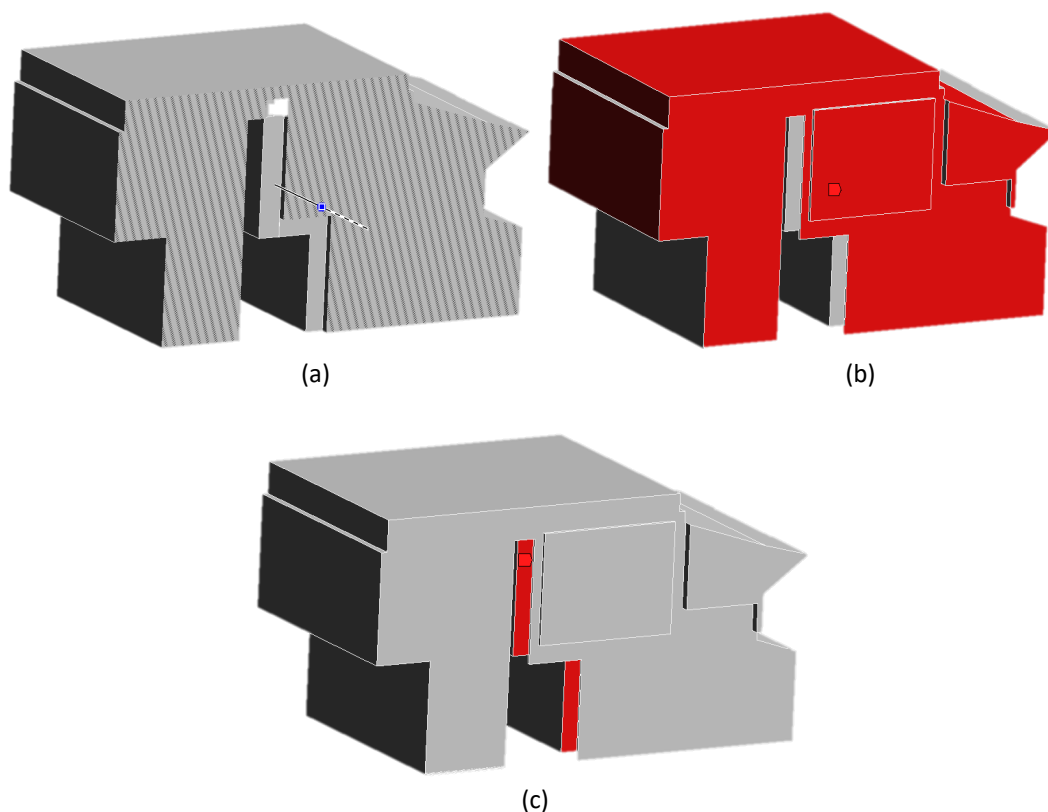


Fig. 2. The boundary condition of car cabin (a) Velocity inlet (b) Wall (c) Outlet

Table 2
 Parameter for boundary condition

Parameter	Dimension
Walls of car	Wall Wall motion=stationary wall Heat flux=0 W.m-2 Discrete phase condition=trap
Mouth of man	Wall Wall motion=stationary wall Heat flux=0 W.m-2 Discrete phase condition= escape
Two men body	Wall Wall motion=stationary wall Heat flux= 0 W.m-2 Discrete phase condition=reflect
Method-pressure velocity coupling	Coupled Pressure=second order Momentum=first order upwind H2O =first order upwind Energy=first order upwind

3. Results

3.1 Grid Independence Test

The grid independence test is an essential procedure for ensuring the accuracy and reliability of simulation results in computational fluid dynamics (CFD) studies. This test involves evaluating different mesh sizes to identify the point at which further refinement does not significantly alter the simulation outcomes, thereby ensuring that the results are independent of grid size. In this study, five different mesh sizes were examined, as listed in Table 3: 516,672 nodes with 2,741,568 elements, 614,481 nodes with 3,301,376 elements, 717,041 nodes with 3,896,155 elements, 811,362 nodes with 4,444,880 elements, and 915,273 nodes with 5,004,162 elements. By comparing the simulation results across these varying mesh sizes, this study aims to determine the optimal grid size that balances the computational efficiency with the result accuracy. The grid independence test confirmed that the selected mesh size was adequate for capturing the critical flow characteristics and particle dispersion patterns within the car cabin, ensuring that the findings were both precise and reliable.

Table 3
 Result of grid independence test (GIT)

Grid	Element size (mm)	Nodes	Element	skewness	Orthogonal
1	7.7523	516672	2741568	0.88998	0.9955
2	1.57	614481	3301376	0.89841	0.99587
3	1.27	717041	3896155	0.89402	0.99735
4	1.13	811362	4444880	0.90326	0.99676
5	1.03	915374	5052242	0.89817	0.99602

3.2 Particle Residence Time

In Figure 3, the particle residence time 1.0 seconds after the driver's cough is illustrated. The simulation showed the initial spread of aerosol particles, indicating a high concentration near the driver's mouth and rapid dispersion throughout the front of the car cabin. This early phase highlights

the immediate impact of the cough, suggesting that droplets remain concentrated close to the source before dispersal begins. The high particle density near the driver's seat is critical because it underscores the potential exposure risk to passengers seated in the front row.

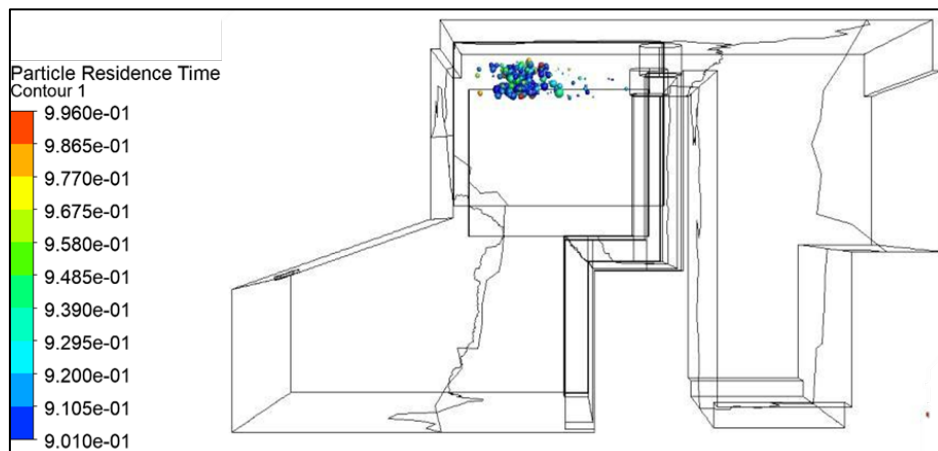


Fig. 3. Particle residence time in min=1.0 s

Figure 4 presents the particle residence time just slightly less than 1.0 seconds, at 0.999 seconds. The simulation showed a significant dispersion of particles from the driver's mouth towards the rear of the car. The decrease in particle density around the driver's seat compared with that in Figure 3 indicates the beginning of particle diffusion throughout the cabin. This figure shows the rapid movement of aerosols within confined spaces, emphasising the need for effective ventilation to mitigate the spread of pathogens.

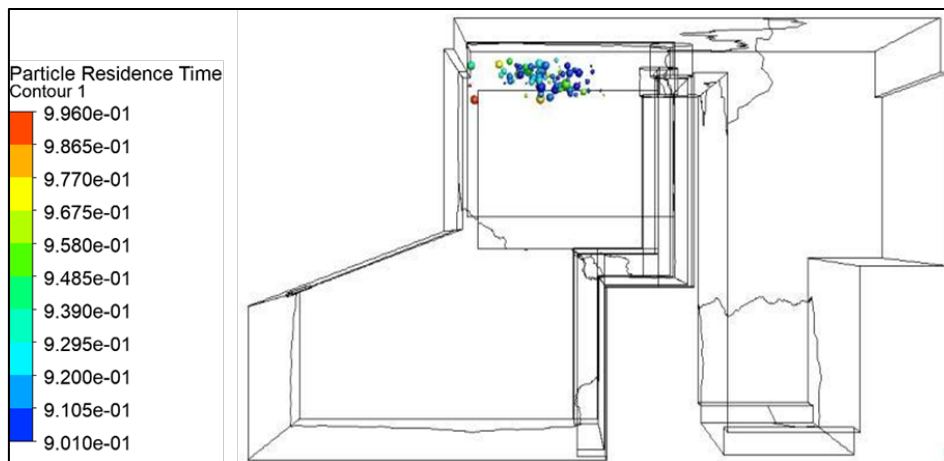


Fig. 4. Particle residence time in min=0.999s

Figure 5 shows the particle residence time at 0.996 s, highlighting the maximum dispersion of the particles within this short timeframe. The particles were more evenly distributed throughout the car cabin, with noticeable concentrations near the rear seat. This even distribution pattern suggests that aerosols can quickly fill the entire space, potentially increasing the risk of inhalation by all passengers regardless of their seating position.



Fig. 5. Particle residence time in max=0.996s

In Figure 6, the simulation at 0.997 s shows the extensive spread of particles throughout the car cabin. The pattern remains consistent with earlier observations, with a further reduction in particle concentration near the driver and increased dispersion towards the rear. This figure reinforces the observation that particles do not remain localised, but quickly spread to all areas within the confined environment, posing a uniform risk of exposure.

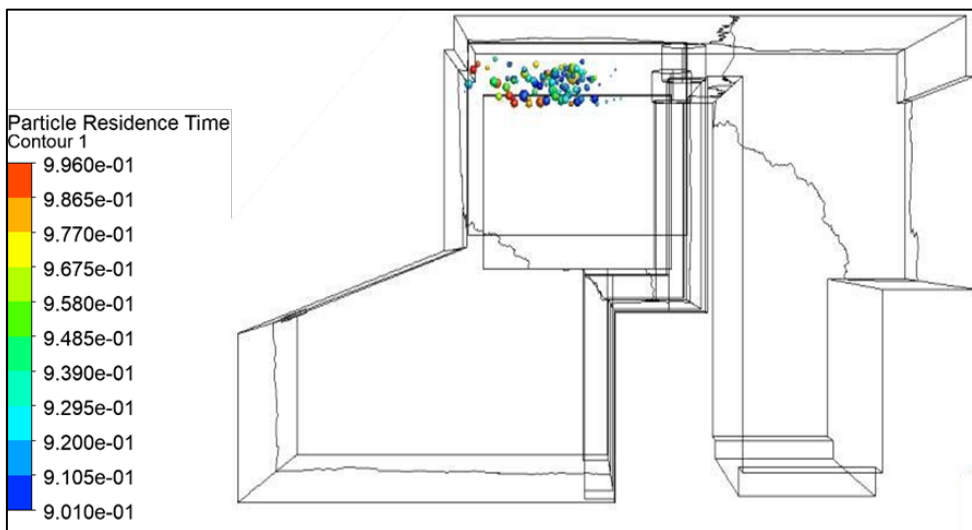


Fig. 6. Particle residence time in max=0.997s

Figure 7 shows the particle residence time at 0.999 s, just shy of the 1-second mark. The distribution pattern shows the persistence of aerosol particles throughout the cabin, with a slight decrease in the overall concentration as the particles settled and diffused. This figure underscores the transient nature of aerosols and the importance of continuous air exchange in reducing particle accumulation and potential exposure over time.

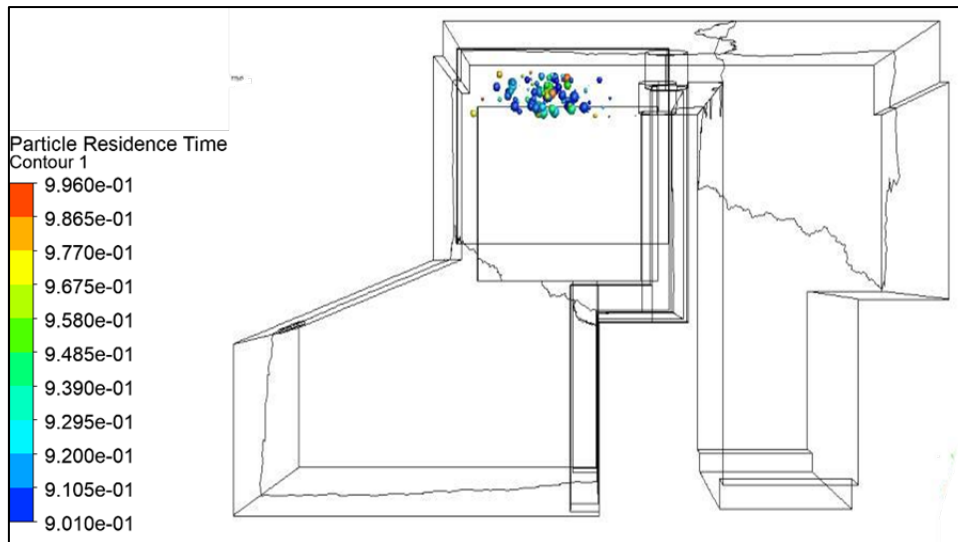


Fig. 7. Particle residence time in max = 0.999s

3.3 Flow Characteristic Aerosol Dispersion in Car Cabin

Figure 8 illustrates the streamline patterns within the car, indicating airflow paths. The simulation showed a predominant counterclockwise circulation driven by the movement of the car and the configuration of open and closed windows. The arrows depict how air enters from the rear-left window and circulates towards the front right, creating a vortex that can trap and transport particles throughout the cabin. This airflow pattern is crucial for understanding how aerosols can be carried and recirculated, thereby affecting the distribution and concentration of potentially infectious particles.

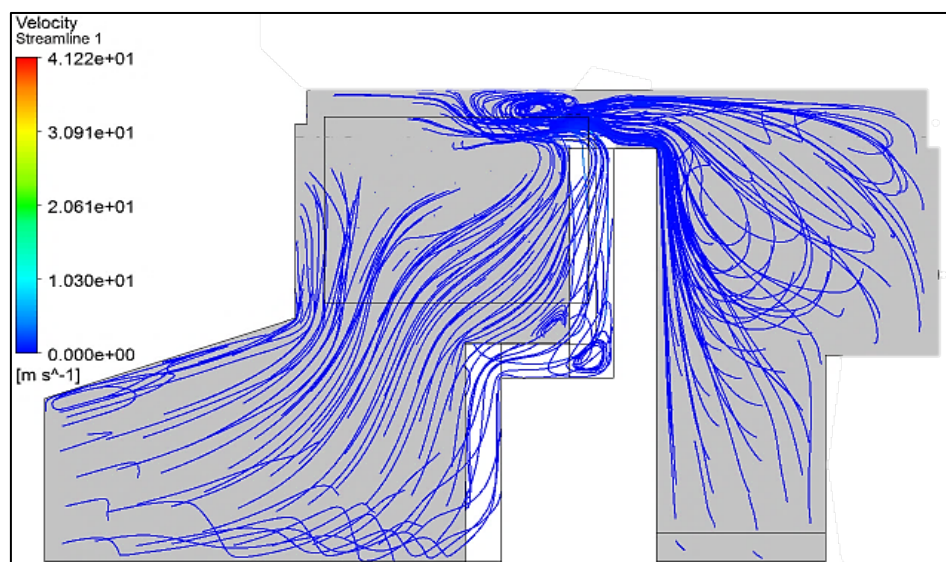


Fig. 8. Streamline pattern in the car interior

The streamlined arrows indicate that the predominant direction of the recirculation zone inside the cabin was counterclockwise (viewed from above). These streamlines represent possible transmission paths, potentially transporting virus-laden droplets or aerosols throughout the cabin and, in particular, from passengers to drivers.

3.4 Velocity Distribution of Aerosol Dispersion in a Car Cabin

Figure 9 shows the velocity distribution within the car, providing insight into the airflow dynamics. The simulation highlighted areas of high and low velocities, corresponding to the entry and circulation of air. Higher velocities were observed near the windows, whereas lower velocities dominated in the central and rear parts of the cabin. This distribution is important to understand how quickly aerosols can be dispersed and diluted. The correlation between high-velocity regions and aerosol spread suggests that enhancing airflow in these areas can help reduce particle concentrations and improve overall air quality.

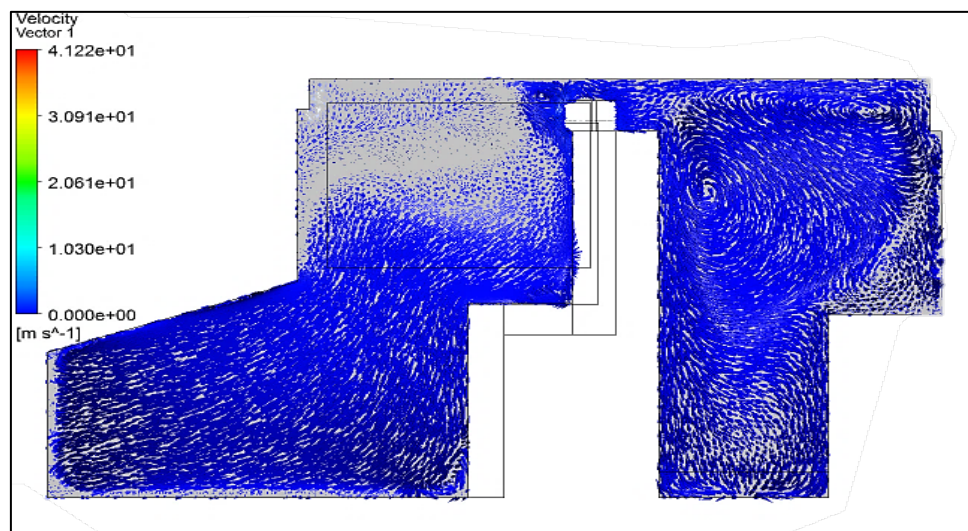


Fig. 9. Velocity distribution in the car cabin

4. Conclusion

This study successfully demonstrated the dynamics of aerosol particles spread within a car cabin following a driver's cough using CFD simulations. The results indicate that aerosol particles can rapidly disperse throughout the confined space, with initially high concentrations near the source and subsequent distribution to all areas within the cabin. The streamline patterns reveal a counterclockwise airflow circulation that facilitates the widespread movement of the particles. Velocity distribution analysis further underscores the role of airflow in determining the particle dispersion and potential exposure risk. These findings highlight the critical need for effective ventilation strategies to mitigate the spread of infectious aerosols in enclosed environments, such as car cabins. Implementing measures to enhance airflow and reduce the particle residence time can significantly lower the risk of exposure to airborne pathogens. This study provides valuable insights into the behaviour of aerosols in confined spaces and underscores the importance of ventilation in ensuring passenger safety during the ongoing COVID-19 pandemic.

Acknowledgement

This research was supported by Universiti Tun Hussein Onn Malaysia (UTHM) through Tier 1 (vot Q449).

References

- [1] Singhal, Tanu. "A review of coronavirus disease-2019 (COVID-19)." *The Indian Journal of Pediatrics* 87, no. 4 (2020): 281-286. <https://doi.org/10.1007/s12098-020-03263-6>

- [2] Salati, Hana, David F. Fletcher, Mehrdad Khamooshi, Jingliang Dong, Kazuhide Ito, Sara Vahaji, and Kiao Inthavong. "Exhaled jet and viral-laden aerosol transport from nasal sneezing." *Aerosol and Air Quality Research* 22, no. 4 (2022). <https://doi.org/10.4209/aaqr.210338>
- [3] Behera, Sachidananda, Rajneesh Bhardwaj, and Amit Agrawal. "Effect of co-flow on fluid dynamics of a cough jet with implications in spread of COVID-19." *Physics of Fluids* 33, no. 10 (2021). <https://doi.org/10.1063/5.0064104>
- [4] Lindsley, William G., Jeffrey S. Reynolds, Jonathan V. Szalajda, John D. Noti, and Donald H. Beezhold. "A cough aerosol simulator for the study of disease transmission by human cough-generated aerosols." *Aerosol Science and Technology* 47, no. 8 (2013): 937-944. <https://doi.org/10.1080/02786826.2013.803019>
- [5] Morawska, Lidia. "Droplet fate in indoor environments, or can we prevent the spread of infection?." In *Indoor Air 2005: Proceedings of the 10th International Conference on Indoor Air Quality and Climate*, pp. 9-23. Tsinghua University Press, 2005.
- [6] Mehta, Sanjay Kumar, Aravindhavel Ananthavel, TV Ramesh Reddy, Saleem Ali, Shyam Bihari Mehta, Sachin Philip Kakkanattu, Pooja Purushotham, and K. B. Betsy. "Indirect Response of the Temperature, Humidity, and Rainfall on the Spread of COVID-19 over the Indian Monsoon Region." *Pure and Applied Geophysics* 180, no. 1 (2023): 383-404. <https://doi.org/10.1007/s00024-022-03205-7>
- [7] Domhagen, Fredrik, Sarka Langer, and Angela Sasic Kalagasidis. "Theoretical Threshold for Estimating the Impact of Ventilation on Materials' Emissions." *Environmental Science & Technology* 58, no. 11 (2024): 5058-5067. <https://doi.org/10.1021/acs.est.3c09815>
- [8] Shereen, Muhammad Adnan, Suliman Khan, Abeer Kazmi, Nadia Bashir, and Rabeea Siddique. "COVID-19 infection: Emergence, transmission, and characteristics of human coronaviruses." *Journal of advanced research* 24 (2020): 91-98. <https://doi.org/10.1016/j.jare.2020.03.005>
- [9] Pirouz, Behrouz, Domenico Mazzeo, Stefania Anna Palermo, Seyed Navid Naghib, Michele Turco, and Patrizia Piro. "CFD investigation of vehicle's ventilation systems and analysis of ACH in typical airplanes, cars, and buses." *Sustainability* 13, no. 12 (2021): 6799. <https://doi.org/10.3390/su13126799>
- [10] Saha, Chayan Kumer, Qianying Yi, David Janke, Sabrina Hempel, Barbara Amon, and Thomas Amon. "Opening size effects on airflow pattern and airflow rate of a naturally ventilated dairy building—A CFD study." *Applied Sciences* 10, no. 17 (2020): 6054. <https://doi.org/10.3390/app10176054>
- [11] Bertone, M., A. Sciacchitano, F. Arpino, C. Canale, G. Cortellessa, G. Grossi, and L. Moretti. "Experimental characterization of the airflow within a car cabin." In *Journal of Physics: Conference Series*, vol. 2509, no. 1, p. 012024. IOP Publishing, 2023. <https://doi.org/10.1088/1742-6596/2509/1/012024>
- [12] Zivich, P. N., M. C. Eisenberg, A. S. Monto, A. Uzicanin, R. S. Baric, T. P. Sheahan, J. J. Rainey, H. Gao, and A. E. Aiello. "Transmission of viral pathogens in a social network of university students: the eX-FLU study." *Epidemiology & Infection* 148 (2020): e267. <https://doi.org/10.1017/S0950268820001806>
- [13] Nazari, Ata, Moharram Jafari, Naser Rezaei, Farzad Taghizadeh-Hesary, and Farhad Taghizadeh-Hesary. "Jet fans in the underground car parking areas and virus transmission." *Physics of fluids* 33, no. 1 (2021). <https://doi.org/10.1063/5.0033557>
- [14] Alexandrov, Alex, Vladimir Kudriavtsev, and Marcelo Reggio. "Analysis of flow patterns and heat transfer in generic passenger car mini-environment." In *9th Annual Conference of the CFD Society of Canada*, vol. 27. 2001.
- [15] Mathai, Varghese, Asimanshu Das, Jeffrey A. Bailey, and Kenneth Breuer. "Airflows inside passenger cars and implications for airborne disease transmission." *Science advances* 7, no. 1 (2021): eabe0166. <https://doi.org/10.1126/sciadv.abe0166>
- [16] Khatoon, Saboor, and Man-Hoe Kim. "Thermal comfort in the passenger compartment using a 3-D numerical analysis and comparison with Fanger's comfort models." *Energies* 13, no. 3 (2020): 690. <https://doi.org/10.3390/en13030690>
- [17] Belkacemi, Djelloul, Mohammad Al-Rawi, Miloud Tahar Abbes, and Boualem Laribi. "Flow Behaviour and Wall Shear Stress Derivatives in Abdominal Aortic Aneurysm Models: A Detailed CFD Analysis into Asymmetry Effect." *CFD Letters* 14, no. 9 (2022): 60-74. <https://doi.org/10.37934/cfdl.14.9.6074>
- [18] Tham, Wei Xian, Normayati Nordin, Azian Hariri, Nurul Fitriah Nasir, Norasikin Mat Isa, Musli Nizam Yahya, and Suzairin Md Seri. "Asymptotic computational fluid dynamic (ACFD) study of three-dimensional turning diffuser performance by varying angle of turn." *International Journal of Integrated Engineering* 11, no. 5 (2019): 109-118.
- [19] Pujari, Aditya R., Sarvgya Kumar, and Pradeep Kumar Sow. "Fluid flow simulation on a Turritella-seashell-like geometry demonstrating its ability as static mixer for inline mixing." *Chemical Engineering Science* 262 (2022): 118031. <https://doi.org/10.1016/j.ces.2022.118031>
- [19] Trimulyono, Andi, Sanggam Tulus Mahatabel Owhaamsorrc Gultom, Eko Sasmito Hadi, and Dedi Budi Purwanto. "Investigation of Sloshing with Vertical and Horizontal Baffle in the Prismatic Tank using Meshfree CFD." *CFD Letters* 15, no. 6 (2023): 115-129. <https://doi.org/10.37934/cfdl.15.6.115129>

- [20] Winarno, Arif, Agung Sugeng Widodo, Gatot Ciptadi, and Atiek Iriany. "The The Effect of Sail Layout on Fishing Vessels Hydrodynamics in The North Coast of Java Using Computational Fluids Dynamic." *CFD Letters* 16, no. 1 (2024): 107-120. <https://doi.org/10.37934/cfdl.16.1.107120>